The Holliday junction in an inverted repeat DNA sequence: Sequence effects on the structure of four-way junctions

Brandt F. Eichman, Jeffrey M. Vargason, Blaine H. M. Mooers, and P. Shing Ho*

Department of Biochemistry and Biophysics, ALS 2011, Oregon State University, Corvallis, OR 97331-7305

Communicated by K. E. van Holde, Oregon State University, Corvallis, OR, December 9, 1999 (received for review November 8, 1999)

Holliday junctions are important structural intermediates in recombination, viral integration, and DNA repair. We present here the single-crystal structure of the inverted repeat sequence d(CCGGTACCGG) as a Holliday junction at the nominal resolution of 2.1 Å. Unlike the previous crystal structures, this DNA junction has B-DNA arms with all standard Watson–Crick base pairs; it therefore represents the intermediate proposed by Holliday as being involved in homologous recombination. The junction is in the stacked-X conformation, with two interconnected duplexes formed by coaxially stacked arms, and is crossed at an angle of 41.4° as a right-handed X. A sequence comparison with previous B-DNA and junction crystal structures shows that an ACC trinucleotide forms the core of a stable junction in this system. The 3′-C·G base pair of this ACC core forms direct and water-mediated hydrogen bonds to the phosphates at the crossover strands. Interactions within this core define the conformation of the Holliday junction, including the angle relating the stacked duplexes and how the base pairs are stacked in the stable form of the junction.

DNA structure | recombination

When genetic information is exchanged, e.g., during recombination between homologous regions of chromosomes or integration of viral DNA into host genomes, the DNA double helix is disrupted. Holliday proposed that the intermediate formed during homologous recombination is a four-way junction (Fig. 1) (1). Similar junctions form in cruciform DNAs extruded from inverted repeat sequences. Recently, the crystal structures of junctions in a DNA–RNA complex (2) and in the sequence d(CCGGGACCGG) (3) have been reported. In the first structure, the DNA/RNA arms are in the A-conformation, whereas in the latter, two G·A mismatched base pairs sit adjacent to the crossover between the duplexes. Here, we present the structure of a Holliday junction in a true inverted repeat DNA sequence d(CCGGTACCGG) in which all of the nucleotides are in B-type helices with Watson–Crick base pairs.

Studies on synthetic four-stranded complexes and DNA cruciforms show that four-way junctions can adopt either an open extended-X or the more compact stacked-X conformations (for a recent review, see ref. 4). In the presence of monovalent cations, the four arms of the junction are extended into a square planar geometry (Fig. 1) to minimize electrostatic repulsion between phosphates. Divalent cations and polyvalent polyamines help shield the phosphate charges (5), allowing the junction to adopt a more compact structure with pairs of arms coaxially stacked as duplexes (Fig. 1) and the duplexes related by ~60° (6–9). A 63° angle is estimated from atomic force microscopy studies on arrays of such junctions (10). During recombination, four-way junctions are resolved by enzymes to complete the process of strand exchange between duplexes. The junctions seen in cocrystals with the resolving enzymes RuvA (11, 12) and Cre (13) are in the extended-X form, whereas T4 endonuclease VII (14, 15) and T7 endonuclease I (16, 17) seem to maintain the relationship of the stacked-X arms.

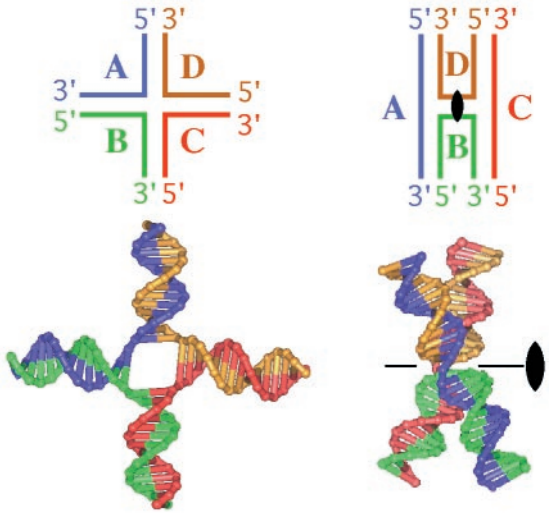

Fig. 1. Conformations of four-way junctions. (*Left*) Association of DNA strands A (blue), B (green), C (red), and D (yellow) to form a junction (*Upper*) with four duplex arms extended in a square planar geometry (extended-X form, *Lower*). (*Right*) These same strands (*Upper*) associated to form the stacked-X structure of the junction, with pairs of arms coaxially stacked as double helices related by 2-fold symmetry (*Lower*).

Despite repeated efforts over the years to crystallize a four-way DNA junction, the recent crystal structures have all been serendipitous. The RNA/DNA junction resulting from studies on an RNA-cleaving DNA motif, or DNAzyme, complexed with its RNA substrate (2) have arms that adopt an A-RNA conformation. The sequence d(CCGGGACCGG) designed to study tandem G·A mismatched base pairs in B-DNA also crystallized as a junction (3); however, the structure around the junction is perturbed by the mismatches. Thus we are left asking what is the structure of a Holliday junction with B-DNA arms and standard base pairs.

We had designed the sequence d(CCGGTACCGG) to study the d(TA) dinucleotide in B-DNA that is a target for the photochemotherapeutic drug psoralen. Surprisingly, four strands of this DNA assembled to crystallize as a four-way junction with all Watson–Crick base pairs. We can thus examine the detailed structure and define the nucleotides and intramolecular interactions that help to stabilize the Holliday junction.

Materials and Methods

Crystallization and X-Ray Data Collection. DNA sequences were synthesized on an Applied Biosystems DNA synthesizer and

Data deposition: The atomic coordinates have been deposited in the Protein Data Bank, www.rcsb.org {PDB ID codes 1DCW [d(CCGGTACCGG)] and 1DCV [d(CCGCTAGCGG)]}.

*To whom reprint requests should be addressed. E-mail: hops@ucs.orst.edu.

The publication costs of this article were defrayed in part by page charge payment. This article must therefore be hereby marked "*advertisement*" in accordance with 18 U.S.C. §1734 solely to indicate this fact.

Table 1. Data collection and refinement statistics

	d(CCGGTACCGG)	d(CCGCTAGCGG)
Data collection		
Resolution range, Å	30.16–2.10	33.81–2.49
Measured (unique) reflections	18370 (6322)	7532 (2009)
Completeness, %*	97.4 (96.7)	98.2 (91.6)
R_{merge}, %*†	4.5 (21.8)	5.2 (41.8)
$\langle I/\sigma_1 \rangle$*	10.6 (2.7)	12.8 (3.1)
Refinement		
Resolution range, Å	8–2.10	10–2.50
No. of reflections (F/σ_F cutoff)	5723 (3.0)	1943 (2.0)
Completeness*	88.9 (68.0)	98.6 (95.4)
R_{cryst} (R_{free})‡	23.0 (31.8)	20.7 (31.7)
DNA atoms (solvent molecules)	808 (92)	404 (23)
Average B-factors, Å^2		
DNA atoms (water atoms)	32.2 (44.6)	55.4 (63.3)
rms deviation from ideality		
Bond lengths, Å (Bond angles, °)	0.017 (1.90)	0.005 (1.00)

*Values in parentheses refer to the highest resolution shell.

†R_{merge} (I) = $\Sigma_{hkl}\Sigma_i|I_{hkl,\,i} - \langle I\rangle_{hkl}|/\Sigma_{hkl}\Sigma_i|I_{hkl,\,i}|$ where I_{hkl} is the intensity of a reflection and $\langle I\rangle_{hkl}$ is the average of all observations of this reflection and its symmetry equivalents.

‡$R_{cryst} = \Sigma_{hkl}|F_{obs} - kF_{calc}|/\Sigma_{hkl}|F_{obs}|$. $R_{free} = R_{cryst}$ for 10% of reflections that were not used in refinement (19). The minimum converged values of R_{free} are reported.

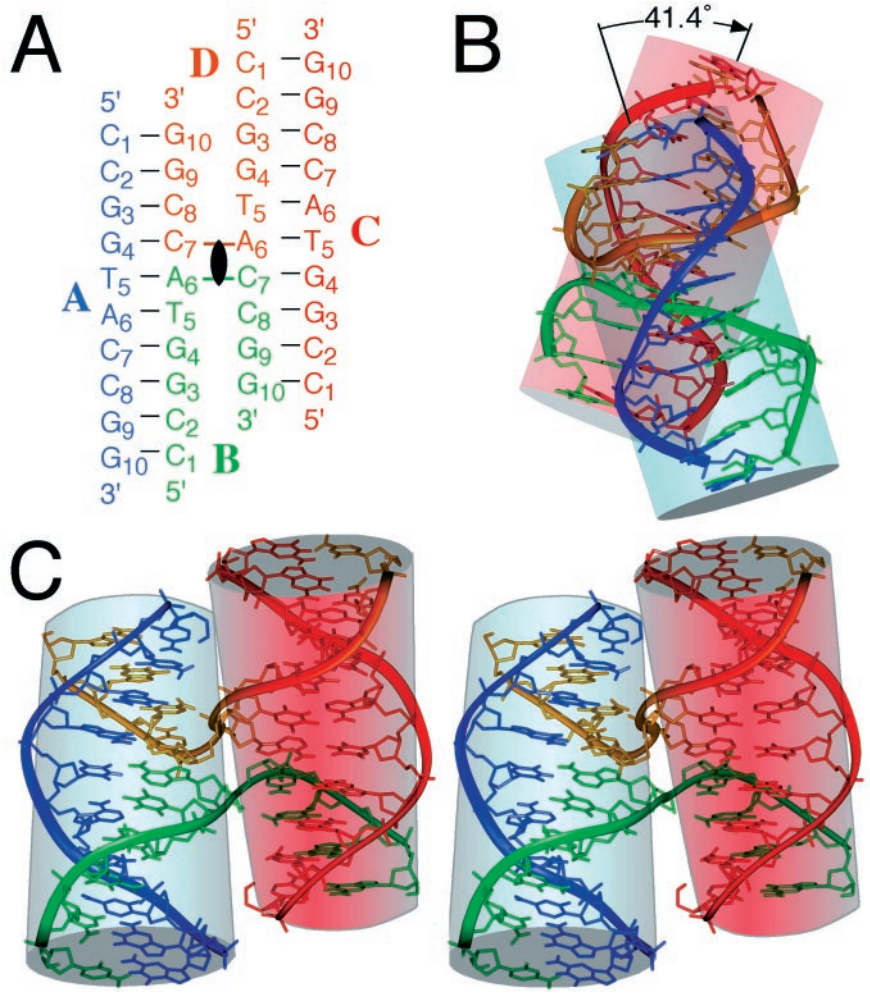

Fig. 2. The Holliday junction structure of d(CCGGTACCGG). (*A*) Four strands of the sequence assemble into the stacked-X conformation of a four-way junction. The strands are numbered 1 to 10 from the 5′ to the 3′ termini. (*B*) View along the Holliday junction. Two duplexes, formed by stacking arms D-A over A-B and C-D over B-C, are related by a right-handed twist of 41.4°. (*C*) Stereoview down the 2-fold axis of the junction. The B and D strands pass from one set of stacked duplexes to the neighboring duplexes.

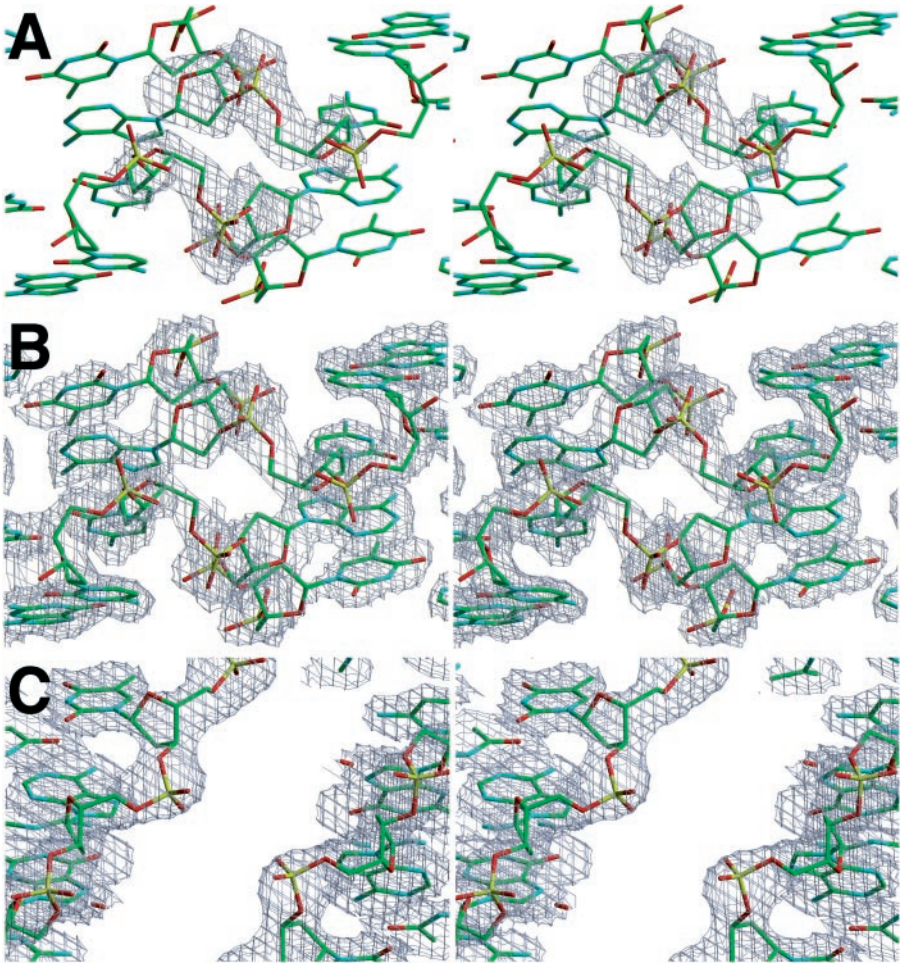

Fig. 3. Stereoview of electron density maps from the d(CCGGTACCGG) and d(CCGCTAGCGG) structures. The atoms are colored as green carbons, red oxygens, blue nitrogens, and yellow phosphoruses. (*A*) $F_o - F_c$ annealed omit map of d(CCGGTACCGG) centered at nucleotides T5 to C8 of strands B and D. The map (contoured at 1.5σ) was calculated with atoms of the phosphoribose backbone of A6 and C7 omitted (but included in the figure for clarity), and the remainder of the DNA subjected to simulated annealing to eliminate model bias. This is indistinguishable from the analogous omit map calculated with a refined noncrossed-over model. (*B*) $2F_o - F_c$ electron density map calculated from the refined model of d(CCGGTACCGG) as a Holliday junction (contoured at 1.0σ). (*C*) $2F_o - F_c$ electron density map of the refined d(CCGCTAGCGG) model as double-stranded DNA. The map is centered at nucleotides T5, A6, and C7, showing the continuity of the trace at the 1.0σ level of each strand.

purified by reverse-phase HPLC. Very thin diamond-shaped crystals of the sequence d(CCGGTACCGG) (dimensions of $300 \times 100 \times 20$ μm^3) were grown at room temperature from solutions containing 0.25 mM DNA, 75 mM sodium cacodylate buffer (pH 7), 15 mM $CaCl_2$, 2.5% 2-methyl-2,4-pentanediol (MPD) and equilibrated against 30% vol/vol MPD. X-ray diffraction data were collected at liquid nitrogen temperatures by using beamline 5.0.2 ($\lambda = 1.1$ Å) at the Advanced Light Source in Berkeley, CA. The crystal is in the monoclinic *C2* space group, with unit cell dimensions $a = 66.5$ Å, $b = 23.5$ Å, $c = 76.9$ Å, and $\beta = 114.8°$. Diffraction images were processed and reflections merged and scaled by using DENZO and SCALEPACK from the HKL package (18). The data were limited to a nominal resolution of 2.1 Å according to $<I/\sigma>$, completeness, and R_{merge} statistics (Table 1).

Similar crystals of the sequence d(CCGCTAGCGG), with dimensions of $400 \times 200 \times 60$ μm^3, were grown at 4°C from solutions containing 0.5 mM DNA, 20 mM sodium cacodylate buffer (pH 7), 50 mM $CaCl_2$, 10% polyethylene glycol (PEG) 200 and equilibrated against 30% vol/vol PEG 200. Data from these crystals were collected at 4°C by using Cu-K_α radiation from a Rigaku (Tokyo) RU H3R rotating anode generator and an R-AXIS IV image plate detector, with images processed and reflections merged and scaled by using D*TREK from Molecular Structure Corp. (The Woodlands, TX) (20). This crystal is also *C2*, with unit cell dimensions $a = 64.1$ Å, $b = 25.9$ Å, $c = 39.9$ Å, and $\beta = 122.0°$.

Structure of d(CCGGTACCGG). This structure was solved by molecular replacement. The native Patterson map showed that two B-type double helices (helical rise = 3.4 Å) were in the asymmetric unit (asu) with the helix axes aligned in the *xy*-plane. Thus, two structures of this sequence as B-DNA were used as the search models in EPMR (21), resulting in correlations of 60% and *R*-factors of 53% for the two molecules in the asu. The models were refined by using X-PLOR 3.851 (22). We observed anisotropic diffraction from these very thin crystals; therefore, anisotropic B-factor scaling was applied to properly weigh the calculated (F_c) to the observed structure factors (F_o) during refinement. The resulting $2F_o - F_c$, $F_o - F_c$ and annealed omit maps showed clean breaks in the electron density between A6 and C7 in each duplex and connectivity across adjacent duplexes. The models were therefore rebuilt with the crossovers of a four-way junction. Minimal noncrystallographic symmetry restraints were subsequently applied between the two crosslinked duplexes. The final values of R_{cryst} and R_{free} converged to 23.0% and 31.8%, respectively (Table 1). These values increase to

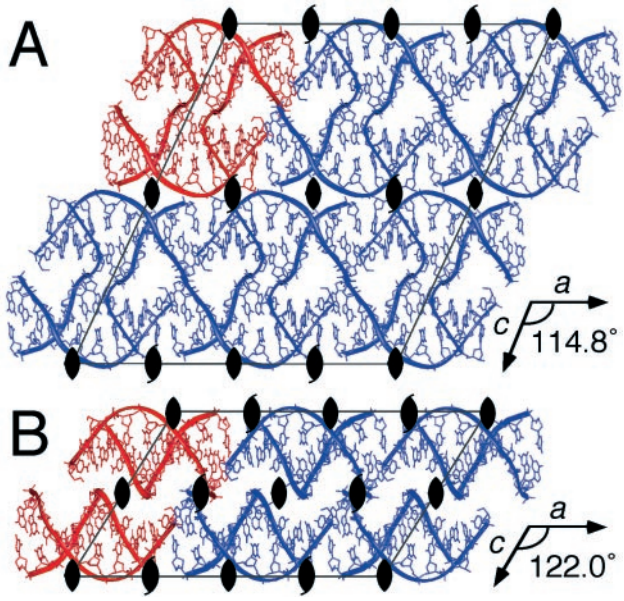

Fig. 4. Crystal packing of the d(CCGGTACCGG) Holliday junction (*A*) and d(CCGCTAGCGG) B-DNA (*B*) structures in the *a*–*c* plane. Four strands in each panel are colored in red, with symmetry related DNAs in blue. In *A*, four DNA strands associate as a single Holliday junction in the asymmetric unit. A 2-fold axis runs through the junction but is slightly shifted from the edge of the unit cell. Because this is a noncrystallographic symmetry axis, the *c*-axis of the d(CCGGTACCGG) unit cell is extended compared with that of d(CCGCTAGCGG). In *B*, the four red strands associate to form two B-DNA duplexes related by true crystallographic 2-fold symmetry.

23.9% and 32.7% when the structure is refined as two non-crossed-over B-DNAs.

Structure Solution of d(CCGCTAGCGG). The structure of d(CCGCTAGCGG) was also solved by molecular replacement. The solution from EPMR (21) was refined by using X-PLOR 3.851 (22), again with anisotropic B-factor scaling applied to F_c during all steps. R_{cryst} converged to 20.7% and R_{free} to 31.7%.

The coordinates and structure factors of d(CCGGTACCGG) and d(CCGCTAGCGG) have been deposited in the Protein Data Bank under accession nos. 1DCW and 1DCV, respectively.

Results

The sequence d(CCGGTACCGG) was observed to crystallize as a four-stranded Holliday junction (Fig. 2) even though it was originally designed to study d(T·A) base pairs in B-DNA. Despite attempts to solve the structure as B-DNA double helices, the electron density maps indicated that the duplexes were connected by the crossed-over strands of a junction. The electron density was consistently observed at all resolution limits to be discontinuous between nucleotides A6 and C7 in one strand of each duplex but to connect these nucleotides across adjacent duplexes. The $F_o - F_c$ maps drawn with the backbone atoms of nucleotides A6 and C7 omitted showed these same connections regardless of whether the structure was refined as two resolved double helices or as a four-way junction (Fig. 3*A*). The structure refined as a junction clearly shows the backbone trace between the adjoining duplex (Fig. 3*B*).

This unusual tracing of the electron density across adjacent duplexes was not an artifact of the crystal lattice or the close approach of the phosphoribose backbone in two B-DNA duplexes. The structure of the nearly identical sequence d(CCGCTAGCGG) places two symmetry related B-DNA duplexes very close to each other (with the phosphates between duplexes approaching 6.2 Å) and in nearly the same orientation as the duplexes of the junction (Fig. 4). The electron density maps could be traced continuously through the backbone of this double helix with no evidence for a junction (Fig. 3*C*). This is further evidence that the sequence d(CCGGTACCGG) had indeed crystallized as a Holliday junction.

The structure of d(CCGGTACCGG) is a junction formed by the crossover of strands between homologous duplexes. In a standard duplex, this would be an inverted repeat sequence. The junction resulting from the assembly of the four identical DNA strands has approximate 2-fold symmetry but with the dyad sitting between A6 and C7 rather than bisecting the sequence. Pairing the complementary nucleotides of the DNA strands A, B, C, and D results in 6-bp A-B and C-D arms and 4-bp C-D and D-A arms.

The A-B arm is coaxially stacked on the D-A arm and B-C stacked on C-D to form the two continuous antiparallel duplexes in the stacked-X form of the junction. The conformation resembles an H with the two arms twisted 41.4° in a right-handed sense (Fig. 2*B*). This angle is not as steep as the ~60° estimated from solution studies and in DNA arrays (6–10) and is not a consequence of the crystal lattice. The sequence d(CCGCTAGCGG)$_2$ crystallizes in a similar lattice but the B-DNA duplexes are related by a 44.1° angle.

The two double helices across the junction are nearly identical to each other, with an rms deviation of 0.2 Å between atoms in the duplexes (0.16 Å for backbone and 0.14 Å for base atoms). Similarly, the twist, tilt, and roll angles between nucleotides are nearly identical in the two duplexes. The two duplexes are also indistinguishable from standard B-DNA, with the exception of the crossovers at the junction. The stacking between base pairs (Fig. 5) in and around the junction is nearly identical to those observed previously in B-DNA. The stacking of the G3·C8 and G4·C7 base pairs within the B-C and within the D-A arms are nearly identical to R·Y over R·Y base pairs (R for purine and Y for pyrimidine bases) in standard B-DNA (23). Furthermore, the stacking between the G4·C7 (of the D-A and B-C arms) and T5·A6 base pairs (of the A-B and C-D arms) across the gap of the junction appears identical to previous R·Y over Y·R stacking motifs. This theme is continued in the hydration of the DNA bases. Each duplex of the structure has a network of waters in the minor groove. Although not as extensive as the spine of waters observed previously in B-DNA (this may be limited by the resolution of the current structure), the networks are continuous through the crossed-over strands. Thus, the stacked arms form B-DNA duplexes with very little disruption in base pairing, base stacking, and solvent interactions by the junction. The only significant deviations from B-DNA are seen as the rotation of the χ-angles of the A8 nucleotides to place them in the high-*anti* conformation and the nearly complete rotation in the β-dihedral angles (P-O5′-C5′-C4′) from an average 146.2° ± 17.0° (calculated from the B-type nucleotides of the current structure) to −157.8° ± 3.2° of the C7 nucleotides. These perturbations extend the phosphates linking the C7 and A8 nucleotides away from their respective duplexes to form the crossover of the junction.

The junction itself is compact and relatively rigid. The temperature factors (B-factors) of the trinucleotides A6-C7-C8 in strands B and D that span the junction and the complementary G3 and G4 nucleotides are generally lower than the remainder of the DNA (Fig. 5). If we accept that B-factors reflect the thermal disorder of atoms in a crystal, the low B-factors of the nucleotides reflect a relatively inflexible junction. This local rigidity can be attributed to specific hydrogen bonds between the C8·G3 base pairs of the B-C and D-A arms and the phosphates at the strands that cross over. The N4 amino group of each C8 is directly hydrogen bonded to the O2P oxygen of the phosphate linking nucleotides A6 and C7 of the crossed-over strands. In addition, a water mediates the interaction

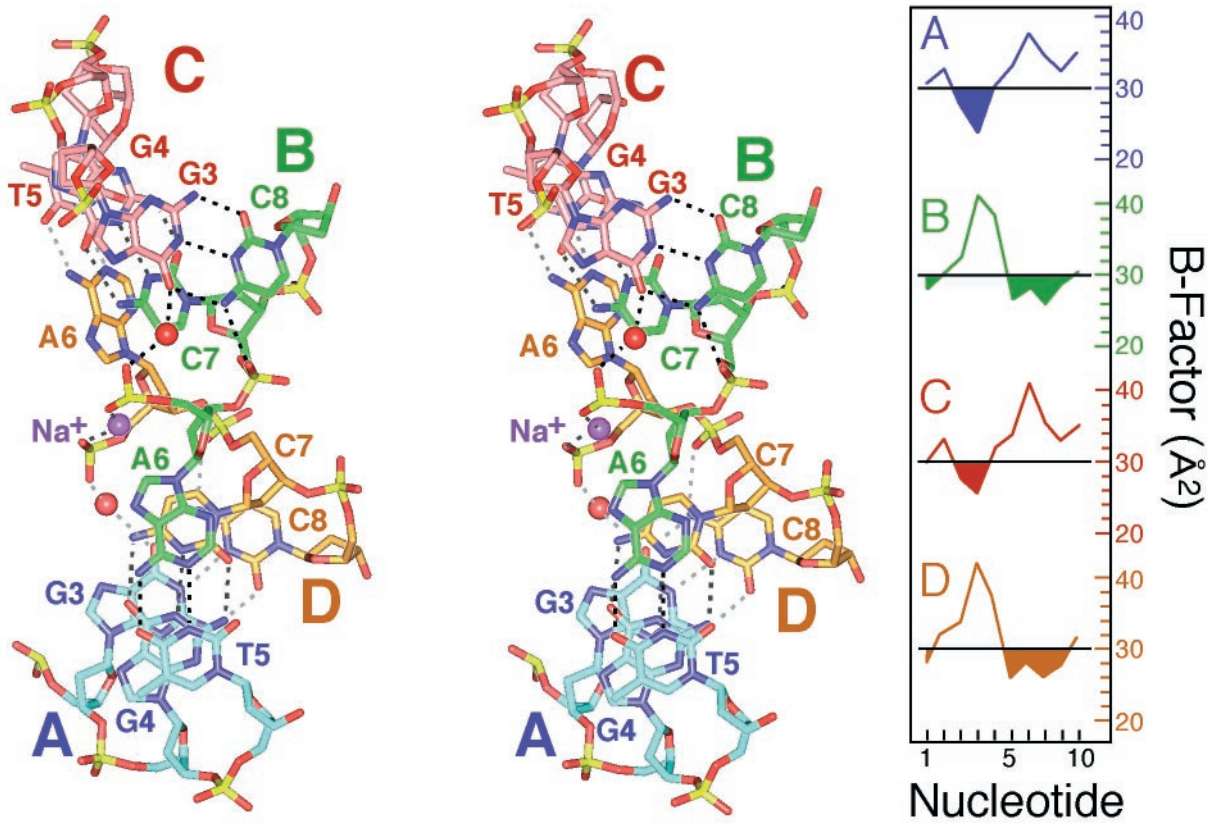

Fig. 5. Structure of the Holliday junction. (*Left*) Stereoview of the crossover at the junction formed by atoms of the G3·C8, G4·C7, and T5·A6 base pairs from strands A (blue carbons), B (green carbons), C (red carbons), and D (yellow carbons). The stacked base pairs of the A-B and D-A arms on the lower half are shown looking down the helix axis. The N4 nitrogens of nucleotides C8 in strands B and D are hydrogen bonded (dashed lines) to the oxygens of the phosphate linking A6 to C7 at the junction crossover. Waters bridging the O6 keto oxygens of guanine G3 in the A and C stands to the 5′-phosphates of A6 are shown as red spheres, whereas the sodium ion that links the 5′-phosphates of the two A6 nucleotides is indigo. (*Right*) Plot of the average B-factor (Å^2) for each nucleotide along strand A (blue), B (green), C (red), and D (yellow). B-factors that are below 30 Å^2 are colored solid. The average B-factor for the DNA model is 32.2 Å^2.

between the O6 keto oxygen of G3 and the O1P phosphate oxygen of adenine A6 (Fig. 5).

The compactness of the junction results in a close approach of four phosphates (within 6.5 Å of each other) at the crossover and thus a highly negative electrostatic potential that must be compensated by counterions. A single well-ordered solvent molecule (B-factor = 18.6 Å^2 vs. an average of 44.6 Å^2 for other added solvent) sits very close (<2.5 Å) to the oxygens of the two A6 nucleotides spanning the junction (Fig. 5). This is closer than

Table 2. Comparison of unique DNA decamer sequences with d(CC)/d(GG) ends and standard nucleotide bases

Conformation	Sequence*	Space group	Reference
Four-way junction	CCGGT**ACC**GG	*C2*	This work
	CCGG<u>GA</u>CCGG	*C2*	3
B-DNA duplex	CCGCT**AGC**GG	*C2*	This work
	CCGGCG**CC**GG	*R3*	25
	CCAGG**CC**TGG	*C2*	26
	CCGCCGG**C**GG	*R3*	27
	CCA**AC**GTTGG	*C2*	28
	CC**AC**TAGTGG	*P3$_2$21*	29
	CCAA<u>GA</u>TTGG	*C2*	30
	CCAAGCTTGG	*P6*	31
	CCATTAATGG	*P3$_2$21*	32

*Nucleotides in the ACC core in the junctions and similar nucleotides in other sequences are in boldface, whereas mismatched base pairs are underlined.

standard hydrogen-bonding distances, suggesting that an Na^+ ion is directly coordinated to the phosphate oxygens. Modeling this as a Ca^{2+} (the other possible cation) increased both R_{cryst} and R_{free}, whereas a Na^+ had no effect on these values. It is well accepted that Na^+ ions are difficult to distinguish from waters at this resolution (24); therefore, we relied on the short distances to the phosphates to make this assignment. We would expect additional ion interactions to help compensate for the phosphate charges, and footprinting studies show that divalent cations such as Mg^{2+} specifically bind to junctions (9). The specificity of these interactions revealed at the nucleotide level, however, may not translate to the atomic level. This may explain why no additional ions were located in the current or the previous (3) mismatched junction structures. Clearly this does not depend on the types of cations present in the crystal, because no well-defined cation complexes could be definitively located at the crossover of the mismatched junction (3), even though the sequence was crystallized in the presence of Mg^{2+} rather than Ca^{2+} solutions.

Discussion

We have solved a structure in which four strands of the sequence d(CCGGTACCGG) assemble to form a Holliday junction. This junction is similar to that previously reported for d(CCGGGACCGG) (3). Both junctions are in the stacked-X conformation, where pairs of helical arms stack coaxially to form nearly continuous criss-crossed duplexes. There are, however, significant differences between the two structures. The current structure has all standard Watson–Crick base pairs, making it rep-

resentative of the intermediate involved in homologous recombination. Furthermore, the junction does not fall on a crystallographic symmetry axis; therefore, each arm around the junction is unique.

Comparing the sequences of similar decanucleotide crystals, we see that an A6-C7-C8 trinucleotide is common to the junction-forming sequences (Table 2). Changing any one of these nucleotides results in a B-DNA duplex. Immediately preceding A6 is either a guanine or thymine; however, because guanine G5 of d(CCGGGACCGG) is mispaired, this position can be any nucleotide. The CC/GG dinucleotide at the 5′ and 3′ termini are common to both the junction and B-DNA sequences, whereas G3 and G4 complement the cytosines of the ACC trinucleotide. This ACC trinucleotide forms the crossover of the four-way junction. The hydrogen bonds from cytosine C8 to an adjacent phosphate at the crossover and the water-mediated hydrogen bonds from G3 to the phosphates of adenine A6 across the junction play important roles in defining the geometry and stability of the junction in both sequences. For example, these well-defined interactions fix the orientation between the two duplexes across the junction and thus account for the 41.4° twist of these duplexes. We therefore define this ACC trinucleotide as the core of the Holliday junction in these crystal systems.

In the structure of d(CCGGGACCGG), the mismatched guanines form unusual hydrogen bonds to cytosines of the flanking C·G base pairs (3), including cytosine C7 of the core ACC trinucleotide. This interbase-pair hydrogen bonding results in a local unwinding of the G4-G5 dinucleotide by 10°. In a B-DNA duplex, G·A mismatches overwind the flanking base pairs (31). We see no distortion to the B-DNA geometry at or near the junction in the present structure. Therefore, the distortions in the d(CCGGGACCGG) structure result from the tandem G·A mismatches and not the junction itself.

The geometry of nucleotides A6 and C7 of the core ACC trinucleotide does not differ significantly from that of B-DNA and, therefore, their role in stabilizing the junction is not entirely clear. Previous biochemical studies on synthetic junctions suggest that base stacking could account for the significance of this AC step in the core. In junctions assembled from four unique DNA strands, there are two different ways to stack four arms into two duplexes. Minor perturbations to the base pairs at the junction have dramatic effects on which arms become coaxially stacked (6). For example, a junction defined by C·G, A·T, T·A, and G·C base pairs, in this order, has the A-B arm stacked on the B-C arm and C-D stacked over D-A. Inverting the C·G to a G·C base pair at the junction results in a duplex with A-B stacked on D-A and B-C on C-D. These effects, which have been quantitated in symmetric sequences by Zhang and Seeman (33), have been attributed to the unique base stacking across the junction. The A6 and C7 nucleotides in the common ACC motif may play a similar role. In addition, the specific hydrogen bonds from the C8·G3 base pair of the ACC core to the phosphates at the crossover help define which stacked isomer is favored in this DNA sequence. Thus, we can start to correlate the sequence-dependent structure with specific structural interactions in the junction.

The structure of the Holliday junction described here and previously (3) is the stacked-X conformation. It is remarkable that both of these crystal structures are so similar to the models previously proposed for junctions assembled with nonhomologous sequences (4). One would expect that a junction between two truly homologous duplexes would migrate and, therefore, would not specifically locate at one position. Migration of the junction through the sequence d(CCGGGACCGG) would presumably be blocked by the two mismatched G·A base pairs. However, in the current structure, we observe that the interactions of the base pairs within the ACC core and with the phosphates at the crossover define the overall conformation of the junction. This includes the angle between the two stacked duplexes and the coaxial stacking of arms in the duplexes within the relatively rigid junction. Thus, this ACC core may help to define a stable Holliday junction that prevents this migration and, therefore, allows the structure to be crystallized.

We thank Prof. P. A. Karplus and his group for helpful suggestions and Drs. K. Henderson and T. Earnest at the Advanced Light Source for help during data collection. This work was supported by grants from the National Science Foundation (MCB-9728240), the American Cancer Society, Oregon Division (J0159880), and the National Institutes of Environmental Health Sciences (ES00210). The x-ray diffraction facility has been supported by the M. J. Murdock Charitable Trust and the Proteins and Nucleic Acids Research Core of the Environmental Health Sciences Center at Oregon State University.

1. Holliday, R. (1964) *Genet. Res.* **5,** 282–304.
2. Nowakowski, J., Shim, P. J., Prasad, G. S., Stout, C. D. & Joyce, G. F. (1999) *Nat. Struct. Biol.* **6,** 151–156.
3. Ortiz-Lombardía, M., González, A., Eritja, R., Aymamí, J., Azorín, F. & Coll, M. (1999) *Nat. Struct. Biol.* **6,** 913–917.
4. Lilley, D. M. J. (1999) in *Oxford Handbook of Nucleic Acid Structure*, ed. Neidle, S. (Oxford Univ. Press, New York), pp. 471–498.
5. Møllegaard, N. E., Murchie, A. I. H., Lilley, D. M. J. & Nielsen, P. E. (1994) *EMBO J.* **13,** 1508–1513.
6. Duckett, D. R., Murchie, A. I. H., Diekmann, S., von Kitzing, E., Kemper, B. & Lilley, D. M. J. (1988) *Cell* **55,** 79–89.
7. Churchill, M. E. A., Tullius, T. D., Kallenbach, N. R. & Seeman, N. C. (1988) *Proc. Natl. Acad. Sci. USA* **85,** 4653–4656.
8. Cooper, J. P. & Hagerman, P. J. (1989) *Proc. Natl. Acad. Sci USA* **86,** 7336–7340.
9. Murchie, A. I. H., Clegg, R. M., von Kitzing, E., Duckett, D. R., Diekmann, S. & Lilley, D. M. J. (1989) *Nature (London)* **341,** 763–766.
10. Mao, C., Sun, W. & Seeman, N. C. (1999) *J. Am. Chem. Soc.* **121,** 5437–5443.
11. Hargreaves, D., Rice, D. W., Sedelnikova, S. E., Artymiuk, P. J., Lloyd, R. G. & Rafferty, J. B. (1998) *Nat. Struct. Biol.* **5,** 441–446.
12. Roe, S. M., Barlow, T., Brown, T., Oram, M., Keeley, A., Tsaneva, I. R. & Pearl, L. H. (1998) *Cell* **2,** 361–372.
13. Gopaul, D. N., Guo, F. & Van Duyne, G. D. (1998) *EMBO J.* **17,** 4175–4187.
14. Bhattacharyya, A., Murchie, A. I. H., von Kitzing, E., Diekmann, S., Kemper, B. & Lilley, D. M. J. (1991) *J. Mol. Biol.* **221,** 1191–1207.
15. Raaijmakers, H., Vix, O., Törö, I., Golz, S., Kemper, B. & Suck, D. (1999) *EMBO J.* **18,** 1447–1458.
16. deMassy, B., Weisberg, R. A. & Studier, F. W. (1987) *J. Mol. Biol.* **193,** 359–376.
17. Dickie, P., McFadden, G. & Morgan, A. R. (1987) *J. Biol. Chem.* **262,** 14826–14836.
18. Otwinowski, Z. & Minor, W. (1997) *Methods Enzymol.* **276,** 307–326.
19. Brünger, A. T. (1992) *Nature (London)* **355,** 472–475.
20. Pflugrath, J. W. (1999) *Acta Crystallogr. D* **55,** 1718–1725.
21. Kissinger, C. R., Gehlhaar, D. K. & Fogel, D. B. (1999) *Acta Crystallogr. D* **55,** 484–491.
22. Brünger, A. T. (1992) *X-PLOR Manual, Version 3.1* (Yale Univ. Press, New Haven, CT).
23. Dickerson, R. E. (1999) in *Oxford Handbook of Nucleic Acid Structure*, ed. Neidle, S. (Oxford Univ. Press, New York), pp. 145–197.
24. Shui, X., McFail-Isom, L., Hu, G. G. & Williams, L. D. (1998) *Biochemistry* **37,** 8341–8355.
25. Heinemann, U., Alings, C. & Bansal, M. (1992) *EMBO J.* **11,** 1931–1939.
26. Heinemann, U. & Alings, C. (1989) *J. Mol. Biol.* **210,** 369–381.
27. Timsit, Y. & Moras, D. (1994) *EMBO J.* **13,** 2737–2746.
28. Privé, G. G., Yanagi, K. & Dickerson, R. E. (1991) *J. Mol. Biol.* **217,** 177–199.
29. Shakked, Z., Guzikevich-Guerstein, G., Frolow, F., Rabinovich, D., Joachimiak, A. & Sigler, P. B. (1994) *Nature (London)* **368,** 469–473.
30. Privé, G. G., Heinemann, U., Chandrasegaran, S., Kan, L.-S., Kopka, M. L. & Dickerson, R. E. (1987) *Science* **238,** 498–504.
31. Grzeskowiak, K., Goodsell, D. S., Kaczor-Grzeskowiak, M., Cascio, D. & Dickerson, R. E. (1993) *Biochemistry* **32,** 8923–8931.
32. Goodsell, D. S., Kaczor-Grzeskowiak, M. & Dickerson, R. E. (1994) *J. Mol. Biol.* **239,** 79–96.
33. Zhang, S. & Seeman, N. C. (1994) *J. Mol. Biol.* **238,** 658–668.